EuroSun2026

FULL-YEAR CASE STUDY ON PLANNED OPERATION OF A PV-COUPLED HIGH-TEMPERATURE THERMAL ENERGY STORAGE REDUCING EMISSIONS AND OPERATING COSTS OF INDUSTRIAL PROCESS HEAT

Nico Oellers (corresponding author), Jonas Schulte, Zahra Mahdi, Nils Kleen and Ulf Herrmann

Solar-Institut Jülich, FH Aachen University of Applied Sciences, Jülich (Germany)

oellers@sij.fh-aachen.de

Summary

Thermal energy storage systems (TESS) provide flexibility in electricity consumption for industrial process heat, allowing the use of renewable electricity during periods of low prices and low carbon intensity. This work applies smartTESS, a modular operational assistance system for TESS, to the energy system of a bakery, comprising a high-temperature TESS, an electric heater, an on-site photovoltaic (PV) field and a gas-fired boiler. One calendar year is simulated at 15-minute resolution on a rolling 24-hour planning horizon that plans against the realised price and carbon-intensity series, with the TESS represented by a dynamic thermocline model and the grid electricity priced at the operator's published 2025 tariff. Results are reported as a sequence of scenarios that adds one component at a time to the same site and quantifies each contribution separately, with exported PV valued under direct-marketing conditions. Against the gas-fired site the full plant reduces annual operating cost by up to 56 % and operating emissions by up to 58 %. By shifting the midday PV generation into the overnight baking process, the TESS enables three quarters of the emission reduction and about a third of the cost reduction. The flexibility of the TESS also qualifies the site for the individual network charge for atypical grid use, a reduced network tariff that increases the cost reduction from 43 to 56 %. Emission-optimised dispatch lowers emissions only marginally below cost-optimised dispatch, because low-price hours in the German market coincide with hours of high renewable infeed.

Keywords: thermal energy storage, operational assistance system, power-to-heat, PV self-consumption, carbon-optimised dispatch, network tariffs

Field of application for the findings: Sustainable Energy Infrastructure and Electrification

Addressed audience: Researchers and engineers working on TESS and energy system optimization

1. Introduction

The growing share of renewable generation changes the operating requirements of industrial energy systems. Fluctuating wind and solar infeed increases volatility on the electricity markets and raises the value of flexibility on the demand side (Kyritsis et al., 2017). A thermal energy storage system (TESS) can provide this flexibility by decoupling electricity consumption from heat demand in time, so that it acts both as a heat supply component and as a demand-side resource (Arteconi et al., 2012). The transition of the European day-ahead market to quarter-hourly trading intervals in October 2025 increases both the potential value of this flexibility and the requirements on its planning, because a plant can follow a 15-minute price signal only if its operation is planned rather than reactive. Industrial process heat is a large and weakly electrified share of final energy demand: for the EU-28 plus Norway, Switzerland and Iceland, Rehfeldt et al. (2018) quantify process heating at roughly 1970 TWh per year. Industrial baking processes require temperatures that exceed the operating range of most commercially available heat pumps, leaving electric resistance heating as an available option for electrification. In bakeries the baking process accounts for the largest share of the site energy demand and follows a pronounced daily production cycle, so the sector is suited for storage-coupled electrification.

High-temperature solid-media TESS are an established concept: one-dimensional models of packed-bed and structured storage are mature (Esence et al., 2019), and a ceramic honeycomb TESS of the type considered here has been characterised experimentally at the Jülich solar tower (Zunft et al., 2011). The open questions concern the operation of such a plant. The first question is how a TESS coupled to an on-site photovoltaic (PV) field should be operated over a full year of historical price, generation and load data in order to reduce operating cost and operating emissions, and whether the two objectives result in the same operation. The second question concerns the contribution of the individual components, since a comparison against a gas-only reference aggregates the effects of three distinct investments: the PV field, the electric heater and the TESS. A third question follows from the comparison itself: the gas price defines the cost reference that grid electricity has to undercut, so its level determines both the extent of grid use by the TESS and the economic value of the electrification.

These questions are addressed with the smartTESS framework, a modular operational assistance system for TESS that for this study includes the simulation of the complete process heat energy system on historical input data. One calendar year is simulated at 15-minute resolution for a PV-coupled high-temperature TESS in a bakery, with the TESS represented by a dynamic thermocline model. The results are reported as a sequence of scenarios that adds one component at a time to the same site, so that the contribution of each component is quantified separately, and all results are reported both with and without the individual network charge for atypical grid use for which the site is qualified by the flexibility of the TESS.

2. The smartTESS framework and the considered energy system

2.1 The smartTESS framework

The smartTESS framework is a modular operational assistance system supporting the economically optimized operation of TESS in renewable energy systems. It combines forecasting, optimization and simulation components in the architecture shown in Fig. 1. Forecasting modules provide predictions of weather conditions, solar generation, heat demand and electricity prices, which feed a hierarchical optimization stage: the long-term optimizer establishes the coarse operating plan and its boundary conditions, the day-ahead optimizer determines the operating schedule within them, and the short-term optimizer refines it on a rolling horizon as forecasts are updated. The simulation core carries the physical models of the plant, including a dynamic thermocline model of the TESS. The framework provides the interface through which the assistance system is to be coupled to the real TESS. A data layer stores results and forecasts, and a reporting layer provides decision support.

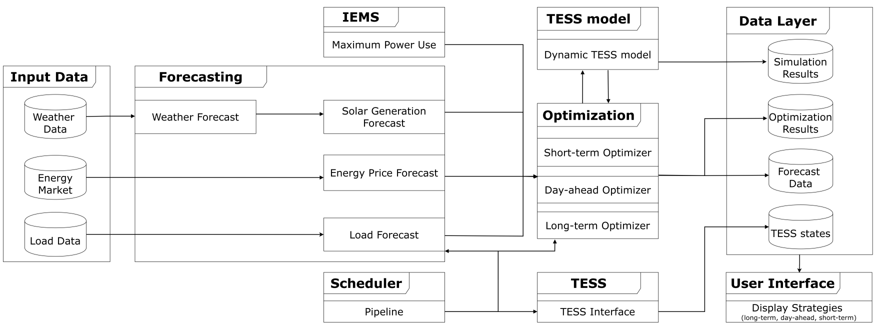

Fig. 1: Simplified architecture of the smartTESS framework.

The present study applies the data layer, the day-ahead and short-term optimization modules, the simulation core and the reporting layer over a full year. The forecasting modules are implemented and characterised separately but are not yet coupled to the controller. The dispatch reported below therefore plans against the realised price and carbon-intensity series and constitutes a perfect-information reference, against which forecast-driven operation will be evaluated once the forecasting layer is coupled.

2.2 The considered energy system

The considered energy system is shown in Fig. 2. It consists of the PV field, the grid connection, the electric heater, the TESS, the gas-fired boiler and the process heat demand of the bakery. The TESS is charged either from grid electricity or from on-site PV through an electric resistance heater, and stored heat is discharged to meet the industrial heat demand. Electricity can also supply the load directly through the same heater, bypassing the TESS and avoiding storage losses. PV covers the concurrent load with priority, and grid electricity does so when its marginal heat cost is below that of gas. A gas-fired boiler covers the residual load.

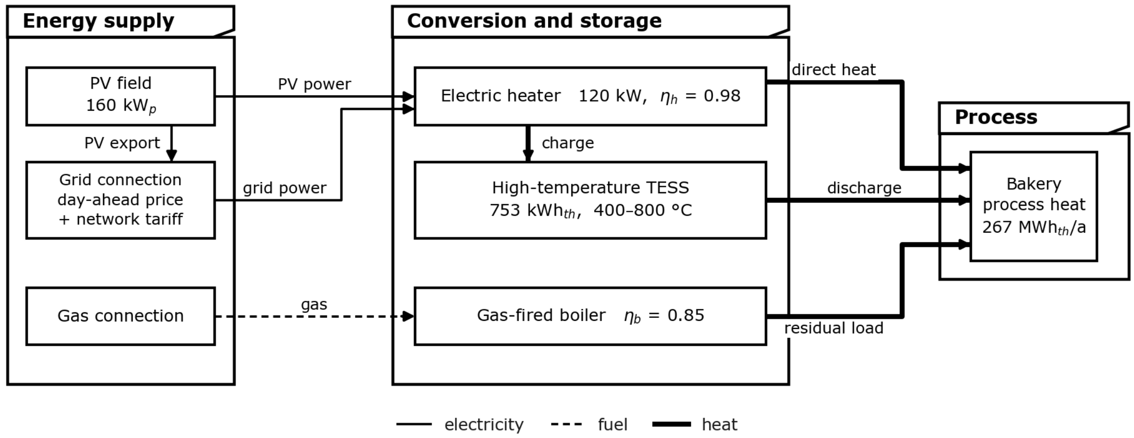

Fig. 2: The considered energy system. PV and grid electricity charge the TESS through an electric heater or supply the load directly through the same heater. The TESS discharges to the industrial heat demand and a gas-fired boiler covers the residual load.

The site is a bakery in Jülich, Germany, with an annual heat demand of 267 MWh_{th} and a peak heat load of 134 kW. The energy system and model parameters are listed in Tab. 1. The plant is sized from the daily production cycle rather than from an economic optimisation. The discharge rating of 170 kW_{th} exceeds the peak heat load of 134 kW, so the TESS alone can cover the load, and the usable capacity of 753 kWh_{th} covers the greater part of one production night. The heater rating of 120 kW allows the usable capacity to be charged within a single midday window.

Tab. 1: Energy system and model parameters.

Quantity	Symbol	Value	Source or note
Rated TESS capacity	$E_{\max}$	753 kWh_{th}	thermocline model (Section 3.1)
Charge inlet temperature	–	800 °C	system design
Process return temperature	–	320 °C	system design
Minimum delivery temperature	–	400 °C	system design
Discharge rating	$\dot{Q}^{\mathrm{dis}}_{\max}$	170 kW_{th}	system design
Heater rating	$P^{\mathrm{ch}}_{\max}$	120 kW	system design
Heater efficiency	η_{h}	0.98	assumption
Boiler efficiency	η_{b}	0.85	assumption
PV peak power	–	160 kWp	system design
Annual heat demand	–	267 MWh_{th}	p90 profile from site measurements
Gas CO_2 intensity	–	240 g/kWh	(Bundesrepublik Deutschland, 2026a)
Gas price	c_{gas}	85.9 €/MWh	H1 2025 (Statistisches Bundesamt (Destatis), 2025)
Feed-in value PV	c_{fi}	61 €/MWh	direct marketing, 0 at negative prices (Section 3.2)
Planning horizon	H	96 steps (24 h)	assumption
Minimum operating state of charge	–	0.05	planning buffer

3. Methods

3.1 System model and dispatch objectives

The TESS is represented by a dynamic one-dimensional thermocline model of the ceramic honeycomb core, implemented in Modelica and exported as a Functional Mock-up Unit (FMU). It resolves the axial temperature profiles of the solid matrix and of the air stream, which are coupled by convective heat exchange, and models axial heat conduction in the solid as well as the heat conduction through the insulation. The model is integrated by the variable-step CVODE solver (Hindmarsh et al., 2005) within every 15-minute step. Charging and discharging are bounded by hysteresis latches on the outlet temperatures: charging ends when the bottom outlet reaches 400 °C and discharging ends when the top outlet falls to 400 °C, so the usable capacity follows from the storage physics at the operating point. Between these latches the model provides a usable window of 753 kWh_{th} at the temperatures of Tab. 1, and the state of charge (SOC) reported below is defined on this window.

Operation is planned by a deterministic look-ahead controller on a rolling 24-hour horizon of 96 steps. At every step it computes the residual load over the horizon after direct PV heating, propagates the required stored energy backwards from the horizon end, and covers that requirement from PV surplus first and from grid electricity in the cheapest admissible steps thereafter. Only the first action of the plan is executed. Within that step the physical dispatch follows a fixed priority order: direct PV supply, TESS discharge, grid electricity and finally the gas-fired boiler.

The two dispatch objectives differ only in the gate that admits grid electricity. The cost-optimised dispatch gates on a break-even against gas,

$$c_{\mathrm{be}}^{\mathrm{ch}} = \frac{c_{\mathrm{gas}}}{\eta_{\mathrm{b}}}\,\eta_{\mathrm{h}}\,\eta_{\mathrm{st}} = 95.1\ \text{€/MWh}, \qquad c_{\mathrm{be}}^{\mathrm{dir}} = \frac{c_{\mathrm{gas}}}{\eta_{\mathrm{b}}}\,\eta_{\mathrm{h}} = 99.0\ \text{€/MWh}, \tag{1}$$

where c_{gas} is the gas price and η_{b} and η_{h} are the boiler and heater efficiencies of Tab. 1. $c_{\mathrm{be}}^{\mathrm{ch}}$ is the break-even for charging the TESS and $c_{\mathrm{be}}^{\mathrm{dir}}$ the one for heating the process directly. The factor η_{h} applies to both paths, since charging runs through the same heater. $\eta_{\mathrm{st}} = 0.96$ is the marginal storage efficiency, obtained from the loss balance across the annual simulations of this study. The dispatch charges only where the full electricity price, that is the day-ahead price plus the regulated adder a of Section 3.2, lies below $c_{\mathrm{be}}^{\mathrm{ch}}$. The emission-optimised dispatch replaces the price gates by carbon gates on the grid CO_2 intensity,

$$g_{\mathrm{be}}^{\mathrm{dir}} = \frac{g_{\mathrm{gas}}}{\eta_{\mathrm{b}}}\,\eta_{\mathrm{h}} = 277\ \text{g/kWh}_{\mathrm{el}}, \qquad g_{\mathrm{be}}^{\mathrm{ch}} = g_{\mathrm{be}}^{\mathrm{dir}}\,\eta_{\mathrm{rt}} = 235\ \text{g/kWh}_{\mathrm{el}}, \tag{2}$$

where $g_{\mathrm{gas}} = 240$ g/kWh is the CO_2 intensity of the gas input including its upstream chain (Bundesrepublik Deutschland, 2026a) and η_{rt} the annual storage-path efficiency, that is the discharged heat per unit of heater output charged into the TESS, which lies between 0.84 and 0.88 across the runs of this study and is 0.85 in the reference run. Grid electricity may supply the process directly when its carbon intensity lies below $g_{\mathrm{be}}^{\mathrm{dir}}$ and may charge the TESS below the stricter gate $g_{\mathrm{be}}^{\mathrm{ch}}$. The price gate values a marginal purchase, for which the standing insulation loss is fixed, and therefore carries the marginal efficiency. The carbon gate instead uses the annual figure: admissible hours are frequent under the emission objective, and a marginal carbon gate of 266 $\text{g/kWh}_{\mathrm{el}}$ admits charging that displaces later PV charging, which in this plant increased emissions and cost at the same time.

3.2 Grid electricity pricing

The regulated adder a on the day-ahead price is the sum of four components,

$$a = a_{\mathrm{net}} + a_{\mathrm{lev}} + a_{\mathrm{tax}} + a_{\mathrm{con}}, \tag{3}$$

where a_{net} is the energy component of the network charge of the local operator, a_{lev} the sum of the statutory levies (the levy under Section 19 of the Electricity Network Charges Ordinance, StromNEV, the offshore grid levy and the levy under the Combined Heat and Power Act), a_{tax} the electricity tax and a_{con} the concession fee. All components are taken from the 2025 price sheet of the local network operator, Stadtwerke Jülich (Stadtwerke Jülich, 2025a). At 120 kW of connected power the site is an industrial customer at low voltage with registering load profile metering (RLM) and fewer than 2500 full-load hours, which admits the electricity-tax relief for manufacturing under Section 9b of the Electricity Tax Act (StromStG) (Bundesrepublik Deutschland, 2026c) and the concession fee rate for contract customers. This gives $a = 100.7$ €/MWh, listed as case V1 in Tab. 2.

The reference case adds an individual network charge for atypical grid use under Section 19(2) sentence 1 StromNEV (Bundesrepublik Deutschland, 2026b), at the statutory floor of 20 % of the published network charge (Bundesnetzagentur, 2026b), applied to the energy charge and the demand charge alike (case V2, $a = 42.6$ €/MWh). The arrangement is not a unilateral entitlement: it is individually agreed with the operator, approved by the regulator, and requires the site's grid draw to avoid the operator's high-load windows substantially and predictably. The statutory floor is the most favourable admissible outcome of that process. Those windows are published for 2025 (Stadtwerke Jülich, 2025b) and are seasonal at the low-voltage level: 08:45–13:00 and 16:30–19:00 in winter (December to February), 11:15–11:45 and 17:15–18:15 in autumn (September to November), and none in spring and summer. The condition is not assumed to be granted but imposed on the simulation as a constraint, in that grid draw is blocked inside these windows in every V2 scenario, and the resulting annual grid draw inside the windows is verified after the run.

Tab. 2: Grid electricity pricing, net values in €/MWh, from the operator's 2025 price sheet. V1 is the applicable industrial tariff, V2 the reference case with the individual network charge. The last column is the annual number of hours in which the day-ahead price plus adder falls below the charging break-even of Eq. (1).

	Case	a_{net}	a_{lev}	a_{tax}	a_{con}	a	h/a below $c_{\text{be}}^{\text{ch}}$
V1	industrial, metered (RLM)	72.6	26.5	0.5	1.1	100.7	182
V2	V1 + Section 19(2) s. 1	14.5	26.5	0.5	1.1	42.6	1568

Two charges fall outside Eq. (3) because they are not marginal: the annual demand charge (39.67 €/kW a below 2500 full-load hours, reduced by the same factor of 0.2 in V2) and the metering charge (78 €/a). The dispatch is planned on the marginal electricity price alone. Both charges therefore lie outside the dispatch signal, the annual peak that sets the demand charge is not managed by the controller, and both are added retrospectively to every cost figure reported below. All cost figures in this paper are annual operating costs, comprising gas procurement, grid electricity procurement including the regulated components and the demand and metering charges, net of feed-in revenue. Capital expenditure is not included.

Exported PV is valued under direct-marketing conditions, since a 160-kWp plant is above the 100-kW threshold for fixed remuneration and sells through the sliding market premium. This mechanism tops the export revenue up to the capacity-weighted statutory reference value of 64.0 €/MWh for a building plant with partial feed-in commissioned in 2025 (Bundesnetzagentur, 2026a), minus a marketing fee of 3 €/MWh. For plants commissioned after February 2025 no support is paid in quarter-hours with a negative day-ahead price (Bundesrepublik Deutschland, 2025), where curtailment is assumed. Curtailment affects only the exported remainder, and the PV generation remains available to the process and to TESS charging in these quarter-hours. In 2025, 23.9 % of this plant's generation falls into such quarter-hours.

3.3 Input data

The simulation is driven by five input series for 2025 at 15-minute resolution: day-ahead prices, PV AC power, grid CO_2 intensity, ambient temperature and the bakery heat load. Day-ahead prices and the generation mix are taken from the Energy-Charts API of Fraunhofer ISE (Fraunhofer ISE, 2026).

The grid CO_2 intensity is the generation-weighted average of the German public net generation, using IPCC 2014 median lifecycle factors per production type (Schlömer et al., 2014). It averages 295 g/kWh over 2025 and ranges from 83 to 530 g/kWh. The lifecycle basis is chosen to match the gas side of the comparison, whose intensity of 240 g/kWh includes the upstream chain as well (Bundesrepublik Deutschland, 2026a). Divided by the heater efficiency, the annual average corresponds to 301 g/kWh$_{\text{th}}$, against 282 g/kWh$_{\text{th}}$ for the gas it would displace. Grid electricity at annual average intensity therefore did not reduce process-heat emissions in 2025, and the carbon gate of Eq. (2) accordingly admits selected hours only.

The PV series is simulated with pvlib (Holmgren et al., 2018) for an array at 30° tilt facing south and scaled to the 160 kWp study plant, with DC-side system losses taken as the PVWatts stack of 14 % (Dobos, 2014) and ERA5 irradiance served by the Open-Meteo archive API (Zippenfenig, 2023). The resulting performance ratio is 0.82 at a specific yield of 1183 kWh/kWp, which is high for the site because 2025 was a year of above-average irradiance.

The heat load rests on measured data from the bakery. Fifty-nine days of metered production were recorded and aggregated into a worst-case daily profile at the 90th percentile of the measured daily consumption (p90), which was extended to the remaining months of the year. The p90 aggregation is a deliberate design choice so that the supply task is assessed against a conservative demand, and the annual demand of 267 MWh$_{\text{th}}$ refers to this profile. Fig. 3 shows the resulting daily cycle and the monthly heat demand. Production takes place overnight: the hourly mean load peaks at 02:00 with 102 kW and falls to 1–7 kW between 12:00 and 22:00, and the monthly demand remains between 21 and 24 MWh$_{\text{th}}$ throughout the year. The profile carries the daily production cycle but no seasonality. The remaining monthly variation of the demand follows from the number of working days and public holidays per month.

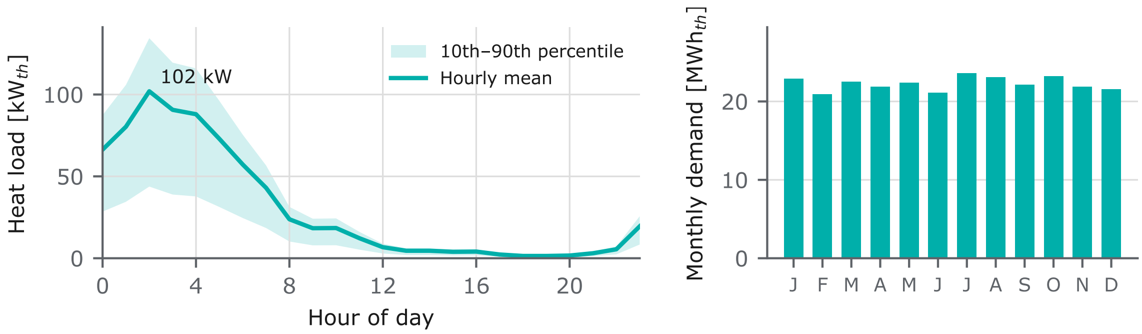

Fig. 3: Heat load of the bakery: daily cycle over the year (left) and monthly heat demand (right).

4. Results and discussion

4.1 Annual performance of the scenario set

The contribution of the TESS can only be quantified if the contributions of the other components are accounted separately. The scenarios of Tab. 3 are therefore built up cumulatively, each adding one component to the same site, so that the difference between two consecutive scenarios quantifies the incremental contribution of the added component. Scenario 0, the existing gas-fired site, is the denominator of every percentage below. Scenario 3 in tariff case V2, that is the cost-optimised dispatch of the full plant with the individual network charge, is the reference case of this study.

Tab. 3: The scenario set. Scenarios 2b, 3 and 4 are run in both tariff cases V1 and V2 of Tab. 2.

Scen.	Adds	Description
0	–	Gas-fired boiler alone, no PV field. The existing site and the denominator of every percentage reported below.
1	PV field	160 kWp added, generation entirely exported. The feed-in revenue offsets part of the gas cost.
2a	Electric heater	120 kW heater added, so that PV can cover the concurrent heat demand directly. No TESS, no grid path, no grid draw.
2b	Grid paths	Both grid paths to that same heater opened, so that grid-direct heating is admitted whenever grid electricity is cheaper than gas. Still no TESS.
3	TESS	Thermocline TESS added, dispatched for cost. Under V2 this is the reference case.
4	CO_2 objective	The same plant dispatched for carbon instead of for cost.

Unmet heat load is exactly zero in every scenario, and grid draw inside the operator's high-load windows is exactly zero in every V2 scenario, which is the condition Section 19(2) sentence 1 requires the site to satisfy. Under V1, where the windows are not enforced, the cost-optimised dispatch places 24 kWh/a of its grid draw inside them and the emission-optimised dispatch 8.7 MWh/a. For the emission-optimised operating point the restriction is therefore a binding constraint, and its year-round observance at uninterrupted heat supply is a property of the planned operation.

Tab. 4: Annual key performance indicators of every scenario.

	Scen. 0	Scen. 1	Scen. 2a	Scen. 2b		Scen. 3		Scen. 4	
KPI	**Gas only**	**PV export**	**PV direct**	**V1**	**V2**	**V1**	**V2**	**V1**	**V2**
Net energy cost [k€/a]	27.0	18.2	17.0	17.0	16.2	11.5	10.7	16.1	12.1
incl. fixed charges [k€/a]	27.0	18.2	17.0	20.4	17.2	15.4	11.8	20.9	13.2
vs. scenario 0 [%]	0.0	−32.5	−36.9	−24.3	−36.2	−43.1	**−56.5**	−22.6	−51.3
Heat cost [ct/kWh$_{th}$]	10.11	6.82	6.38	7.65	6.45	5.75	**4.40**	7.82	4.93
CO_2 emissions [t/a]	75.4	75.4	67.8	67.8	65.2	34.4	32.0	31.3	31.5
vs. scenario 0 [%]	0.0	0.0	−10.1	−10.2	−13.6	−54.5	−57.5	**−58.5**	−58.3
Heat met by TESS [%]	0.0	0.0	0.0	0.0	0.0	44.5	50.3	57.5	56.5
PV to TESS [MWh$_{el}$/a]	0.0	0.0	0.0	0.0	0.0	143.0	140.1	135.7	136.1
Grid to TESS [MWh$_{el}$/a]	0.0	0.0	0.0	0.0	0.0	1.1	21.0	46.7	43.2
Total grid draw [MWh$_{el}$/a]	0.0	0.0	0.0	0.5	22.5	1.5	28.4	65.6	61.8
of which in high-load window [MWh$_{el}$/a]	0.0	0.0	0.0	0.0	0.0	0.02	0.0	8.7	0.0
mean intensity of grid draw [g/kWh]	–	–	–	107	157	110	148	184	184
Demand charge [€/a]	0	0	0	3404	952	3784	952	4760	952
Equivalent full cycles [1/a]	0.0	0.0	0.0	0.0	0.0	157.8	178.6	204.1	200.5

Tab. 4 lists the annual result of every scenario, and Fig. 4 resolves the cost and emission reduction of the full plant into the contributions of the individual components. On the emission side the attribution is unambiguous. The PV field leaves the emissions of the process unchanged, because the boiler consumption remains 314 MWh of gas and the PV generation is exported completely. Adding the heater, so that PV can serve the concurrent heat demand, removes 7.6 t CO_2/a, corresponding to an electrically supplied share of 10.1 % of the heat demand. The constraint is temporal: the bakery produces overnight while the PV field generates around noon. Opening the grid paths to the same heater removes a further 2.7 t CO_2/a from 22.5 MWh_{el}/a of grid-direct heating. The TESS then removes 33.1 t CO_2/a, which is 76 % of the total reduction of 43.4 t between scenario 0 and the reference case.

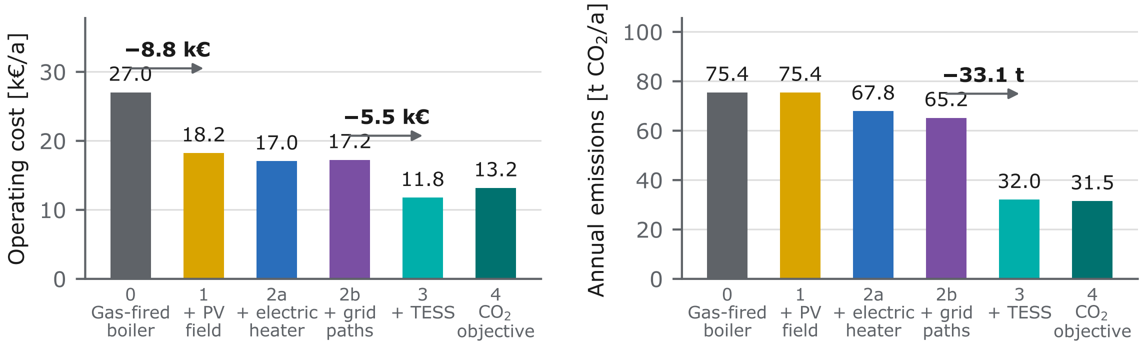

Fig. 4: The scenario set in annual operating cost (left) and annual emissions (right), reference tariff case V2.

On the cost side the largest single contribution is the PV field, which reduces the annual operating cost by 8.8 k€/a through export revenue without affecting the process. Cost attribution depends on the order in which the components are installed, so the direct comparison is reported as well. In the comparison with scenario 2b, which differs from the reference case only in the presence of the TESS, adding the TESS reduces the annual operating cost by 31.8 % and the emissions by 50.8 %, in absolute terms by 5.5 k€/a and 33.1 t CO_2/a. Under direct-marketing conditions self-consumption is considerably more valuable than export, and the TESS is the component that converts exported into self-consumed energy.

The emission attribution is order-dependent as well. In the scenario sequence the PV field is added first and the TESS last, so the TESS step is credited with the full effect of the combination of the two, namely 76 % of the total reduction. In the reverse order, where the same TESS and heater operate on grid electricity alone and the PV field is added last, the TESS accounts for 25 % (10.8 t) and the PV field for 75 %. The two orderings together identify the mechanism: the TESS alone reduces emissions only marginally, because average grid electricity is no cleaner than the gas it displaces, and the PV field alone leaves the process emissions unchanged. Only their combination, midday PV generation shifted by the TESS into the overnight production, removes the 33.1 t attributed to the TESS step.

4.2 Energy flows and seasonal behaviour of the reference case

The origin of the TESS contribution is visible in the energy flow shares, which do not change qualitatively with the tariff. The TESS is charged with 140.1 MWh_{el}/a from the on-site PV field and with 21.0 MWh_{el}/a from the grid, while a further 26.9 MWh_{th}/a of PV generation supplies the process directly through the heater. The TESS therefore shifts self-generated energy from midday into the production hours rather than performing day-ahead price arbitrage. Grid charging is the smaller, complementary part. It is admitted only while the full electricity price lies below the charging break-even of Eq. (1), in 182 h/a under V1 and 1568 h/a under V2 (Tab. 2), and under V2 additionally outside the blocked high-load windows. The tariff case therefore determines the grid share of the charge mix: grid charging into the TESS rises from 1.1 MWh_{el}/a under V1 to 21.0 MWh_{el}/a under V2, while PV charging remains at 143.0 and 140.1 MWh_{el}/a respectively.

This mechanism is strongly seasonal, which is not visible in the annual figures and is resolved in Fig. 5. From April to September the electrically supplied share of the monthly heat demand lies between 76 and 91 % and the boiler covers only a residual load, whereas in December and January the same plant reaches 29 % and the boiler covers the remainder. The TESS bridges the daily cycle rather than the season, so the annual saving is composed of a largely electrified summer and a largely gas-fired winter. Since the load profile carries no seasonality, this variation is driven entirely by PV availability.

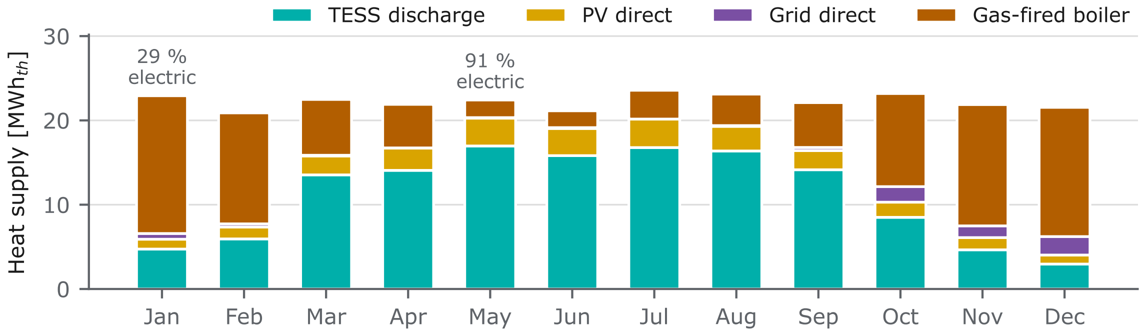

Fig. 5: Monthly heat supply of the reference case by source.

Fig. 6 shows the same behaviour at 15-minute resolution. In summer the TESS completes daily full cycles on PV alone, with the heater operating at its 120 kW rating around noon and the boiler nearly idle. In winter the low PV yield leaves most of the load to the boiler, and grid charging occurs only in isolated night hours below the break-even.

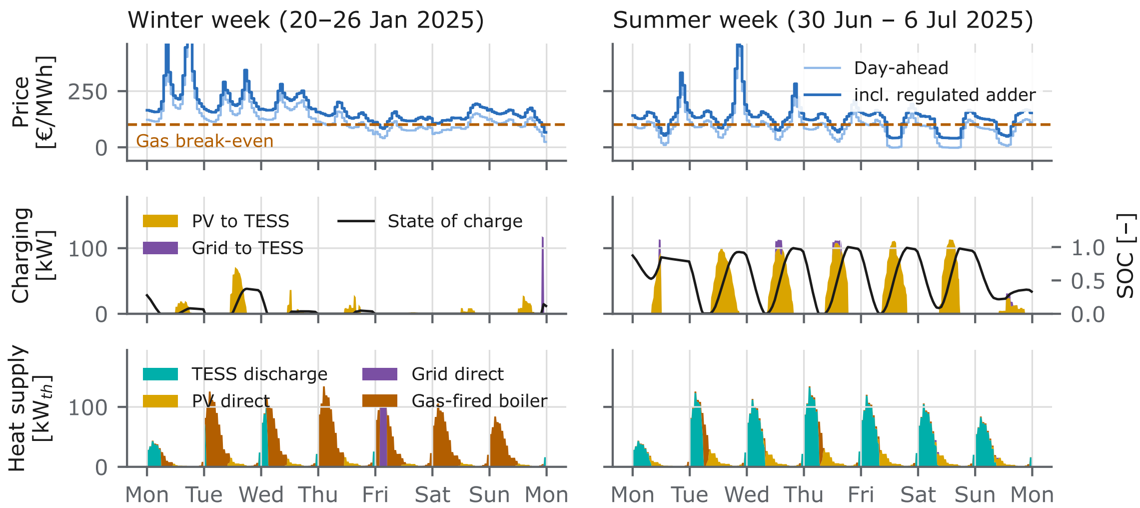

Fig. 6: Cost-optimised dispatch in the reference tariff case for a winter (left) and a summer (right) example week.

4.3 Influence of the network tariff regime

The individual network charge reduces the annual operating cost of the cost-optimised plant by 3.6 k€/a and that of the emission-optimised plant by 7.7 k€/a, as shown in Fig. 7. Both values are of the same order as the 5.5 k€/a contribution of the TESS itself, so the tariff regime and the TESS influence the cost result to a comparable degree. In relative terms the reference case saves 43.1 % against scenario 0 without the individual network charge and 56.5 % with it, while the emission-optimised dispatch saves 22.6 and 51.3 % respectively.

The two objectives obtain this value through different mechanisms. The cost-optimised dispatch draws little grid electricity, so the reduced energy charge accounts for only 0.8 k€/a and 78 % of its improvement results from the reduced demand charge. For this operating point the individual network charge acts primarily on the connection cost. The emission-optimised dispatch uses the grid more, so the reduced energy charge accounts for 3.9 k€/a or 51 % of its improvement. The two mechanisms of Section 19(2) therefore address two different operating points of the same plant.

The demand charge is the larger of the two mechanisms here. Because the dispatch sees only marginal prices, it charges at the full heater rating whenever a quarter-hour clears the break-even. Every scenario that uses the grid therefore sets an annual peak of 95 to 120 kW regardless of how little energy is drawn. Under V1 the cost-optimised dispatch draws only 1.5 MWh/a of grid electricity at 16 full-load hours, so its demand charge of 3.8 k€/a corresponds to about 2.5 €/kWh of the energy drawn. For this operating point the demand-charge share therefore marks the upper end of the tariff value, since a dispatch that also managed the annual peak

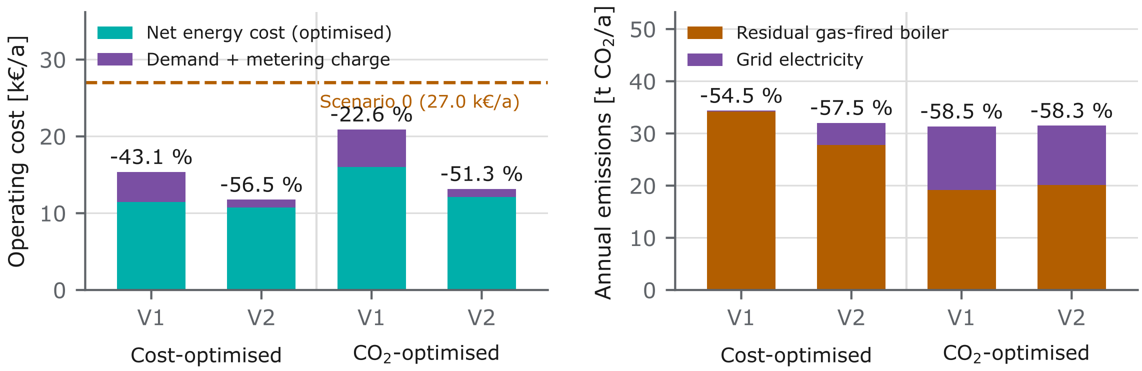

Fig. 7: The four TESS operating points in operating cost (left) and in emissions (right). The cost bar is split into the energy cost addressed by the dispatch and the fixed charges outside the dispatch signal, the emission bar into remaining gas-fired boiler and grid electricity.

would reduce it under V1. Scenario 2b quantifies this consequence: under V1, opening the grid paths raises the annual operating cost from 17.0 to 20.4 k€/a although the site draws only 0.5 MWh of grid electricity, because this draw sets an annual peak of 86 kW and thus a demand charge of 3.4 k€/a. Power-to-heat without a TESS is therefore the configuration most heavily burdened by the German demand charge under such marginal-cost operation.

The reduction is conditional on shifted operation. Zero grid draw inside the high-load windows is reached only in the constrained runs, and in these runs the heat demand is met completely, so the qualification for the individual network charge is a demonstrated property of the planned operation under the realised input series rather than an assumption. It constitutes a permanent operational obligation, verified retrospectively on the measured load profile, and maintaining it over a full year at uninterrupted heat supply is a task for an operational assistance system rather than for manual operation.

4.4 Comparison of cost-optimised and emission-optimised dispatch

Replacing the price gates by carbon-intensity gates changes the operation of the plant. The TESS then charges whenever grid electricity satisfies the loss-aware carbon charging gate of Eq. (2), which in 2025 held for 2928 h/a or 33 % of the year, grid charging into the TESS roughly doubles from 21.0 to 43.2 MWh_{el}/a, and equivalent full cycles rise from 178.6 to 200.5 per year.

The emission balance changes only marginally. The emission reduction increases from 57.5 to 58.3 % relative to scenario 0, corresponding to 0.6 t CO_2/a, at an additional operating cost of 1400 €/a or roughly 2500 € per tonne. Under V1 the same switch reduces emissions by 3.0 t at about 1800 € per tonne. Compared with the 33.1 t removed by the TESS itself, the choice of dispatch objective is a second-order effect.

The reason is that the price signal already selects hours of low carbon intensity. The electricity the cost-optimised dispatch procures averages 110 g/kWh under V1 and 148 g/kWh under V2, whereas the emission-optimised dispatch procures at 184 g/kWh and achieves its marginally lower total through a higher degree of electrification, at 61.8 against 28.4 MWh_{el}/a of grid draw. For this plant, cost-optimised dispatch is therefore close to emission-optimised dispatch.

4.5 Sensitivity to the gas price

The gas price sets both terms of the comparison at once, since it scales the reference cost and, through Eq. (1), the width of the charging window. The reference gas price of 85.9 €/MWh is the Destatis band average for German non-household customers in the 1000–10 000 GJ/a band in the first half of 2025 (Statistisches Bundesamt (Destatis), 2025), and the annual gas input of 314 MWh of the considered bakery lies within that band. Fig. 8 sweeps the gas price from 60 to 140 €/MWh at otherwise unchanged configuration. Each grid point is one annual simulation with the thermocline model of Section 3.1, and the points at the reference gas price are the cost-optimised runs of Section 4.1. Three effects can be distinguished.

The grid use of the TESS is governed by the gas price, which the lower panels of Fig. 8 resolve. In the reference tariff case the admissible charging window widens from 1205 to 6446 h/a across the sweep, grid charging into the TESS grows from 14.3 to 88.9 MWh_{el}/a, the TESS coverage of the heat demand rises from 48.3 to 70.8 %

at 171 to 251 equivalent full cycles, and the electrified share of the heat demand rises from 60 to 92 %. The gas price is therefore the main determinant of how strongly the TESS participates in the electricity market, while its PV-driven base operation is price-independent.

The cost reduction is robust in the reference tariff case, varying between 54.9 and 60.3 % across the sweep: a higher gas price raises the reference cost but also widens the charging window, so residual gas is replaced by grid electricity and the two effects nearly cancel. Without the individual network charge the cost reduction does not increase steadily with the gas price but reaches a minimum of 41.6 % at 100 €/MWh. The minimum follows from the demand charge: set by the annual peak, it is incurred almost in full with the first admitted grid hours, whereas the fuel-cost benefit grows only gradually with the window. Below the reference gas price the V1 charging window is nearly empty (51 to 182 h/a): at 60 €/MWh the plant draws no grid electricity at all, carries no demand charge and even exceeds the V2 result, while at the reference gas price it draws 1.5 MWh/a at a peak of 95 kW. From 100 €/MWh onwards it charges at the full 120 kW heater rating and pays the full demand charge of 4.8 k€/a. The demand-charge step begins just above the Destatis band average, so the applicable tariff V1 shows its least favourable cost result in the range directly above the reference gas price.

The emission reduction is insensitive to the gas price only as long as the charging window remains moderate. Between 60 and 100 €/MWh it varies by less than 2.5 percentage points in both tariff cases, because it is carried by self-consumed PV and does not depend on the gas price. Above 100 €/MWh the break-even of Eq. (1) admits increasingly many grid hours whose carbon intensity approaches that of the gas they displace, so the additional grid electricity reduces cost but hardly reduces emissions. The thermal losses of the TESS amplify this effect, since part of every grid-charged kilowatt-hour is lost before delivery. In the reference case the emission reduction falls from 58.3 % at 100 €/MWh to 49.4 % at 140 €/MWh while the cost reduction still rises, and at 120 €/MWh and above it lies below the value of tariff case V1 with its narrower charging window. A high gas price therefore improves the economics of the TESS but reduces the emission benefit of cost-optimised dispatch.

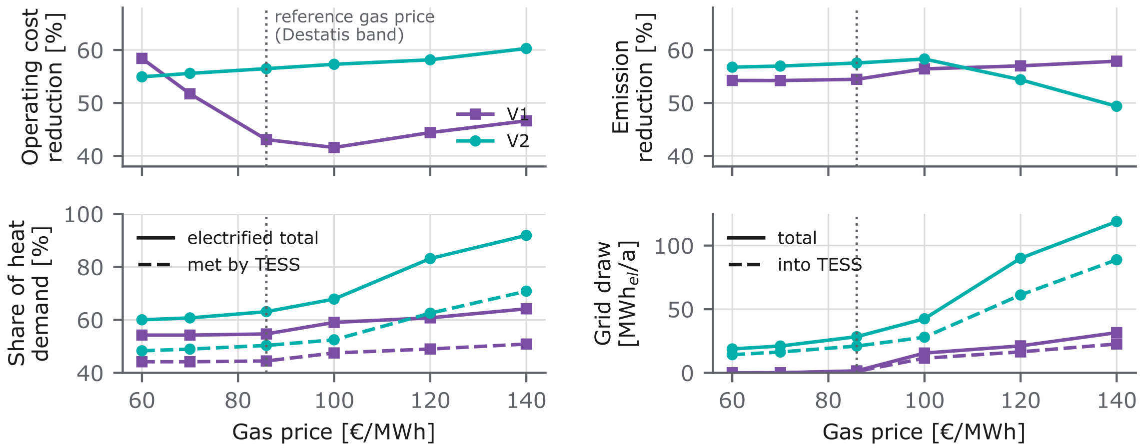

Fig. 8: Sensitivity to the gas price for both tariff cases: operating cost and emission reduction against scenario 0 (top), electrified and TESS-supplied share of the heat demand and annual grid draw (bottom). Dotted: the reference gas price (Destatis band average).

4.6 Scope and validity of the results

The savings reported here are operating costs against a gas-fired boiler reference and contain no capital expenditure, so the figures are not an investment appraisal.

Two accounting conventions increase the reported emission reduction. Electricity generated and consumed on site is booked at zero emissions, which is the convention of Annex 9 of the German Building Energy Act (Bundesrepublik Deutschland, 2026a) and of site-level reporting, but it is not consistent with the lifecycle grid factor used here. If the self-consumed PV generation were accounted at the IPCC lifecycle median of 45 g/kWh, the emissions of the reference case would increase by 7.5 t CO_2/a and its emission reduction would decrease from 57.5 to 47.5 %. The emission accounting is furthermore attributional: PV generation consumed on site is not exported and therefore no longer displaces grid generation elsewhere, and this displacement is not credited. Valued at the concurrent grid intensity, the forgone export amounts to 35.2 t CO_2/a. On that system-level basis, measured against scenario 1 so that the PV field is common to both sides, the TESS step remains the dominant contribution at 53 %.

Further limitations concern the input data and the controller. The look-ahead controller plans against the realised price and carbon-intensity series, so the reported savings constitute a perfect-information reference. Its admission gates are static heuristics that value a stored kilowatt-hour with a constant efficiency and represent neither the holding time of the stored energy nor the displacement of later PV charging. The demand charge is not part of the dispatch signal at all: the controller does not manage the annual peak and charges at the full heater rating, so the demand-charge share of the reported tariff effect is specific to this marginal-cost dispatch. An optimization of the storage trajectory that prices these effects, including the annual peak, endogenously is the corresponding next step of the framework. The day-ahead price is genuinely quarter-hourly only from 1 October 2025, and the PV yield of 1183 kWh/kWp represents an above-average year at this site.

5. Conclusion and outlook

A PV-coupled high-temperature TESS in a bakery was simulated for one full year with the smartTESS framework, with the TESS represented by a dynamic thermocline model. In the reference case, the cost-optimised dispatch in tariff case V2, the planned dispatch supplies 50.3 % of the annual process heat from the TESS at 178.6 equivalent full cycles, without unmet heat load and without grid draw inside the network operator's high-load windows. This demonstrates that the simulation and dispatch layers of the framework operate the plant admissibly over a full year under real input series.

The cumulative scenario set separates the contributions of the PV field, the electric heater, the grid connection and the TESS, with exported PV valued under direct-marketing conditions. Against the gas-fired site the full plant reduces annual operating cost by 56.5 % and operating emissions by 57.5 %, at an operating heat cost of 4.40 against 10.11 ct/kWh$_{th}$. The PV field is the largest single contribution on the operating cost side and leaves the emissions of the process unchanged. Adding the electric heater and its grid paths on top of the PV field removes 10.3 t CO_2/a but reaches only 18 % of the heat demand. The TESS reduces emissions by a further 33.1 t CO_2/a and the operating cost by 5.5 k€/a, enabling 76 % of the emission reduction and about a third of the cost reduction. This attribution is order-dependent and site-specific, but the underlying mechanism is unaffected: the TESS couples on-site generation to the process demand. Dispatching the TESS for carbon rather than for cost removes a further 0.6 t CO_2/a at about 2500 € per tonne, and only if the carbon gate accounts for the storage losses, so economic optimization of this plant is already close to carbon-optimal.

The cost result depends on the tariff regime in addition to the plant. The individual network charge for atypical grid use contributes 3.6 to 7.7 k€/a depending on the objective under the marginal-cost dispatch considered, of the same order as the TESS contribution. It requires grid draw to be kept outside the operator's high-load windows throughout the year. The emission reduction is carried by the TESS and is essentially unaffected by the tariff. This asymmetry is the central operational finding: the TESS decarbonises the process, whereas the economic viability of the electrified plant depends on the gas contract and on the network charge regime.

Within the smartTESS development, this study establishes the simulation and dispatch layers as operational. The next steps extend the framework in four directions. The first is coupling the price, generation and load forecasts into the controller and quantifying the loss against the perfect-information reference. This evaluation includes varied levels of forecast uncertainty. The second is generalising the plant interface so that further heat sources and sinks can be combined with the TESS as building blocks. The third is extending the optimization layer beyond the rule-based planner, replacing the static admission gates by an optimization of the storage trajectory with the demand charge inside the planning objective, and a comparison against mathematical programming and reinforcement-learning dispatch. The fourth is testing the assistance system against the real TESS through the framework's interfaces.

References

A. Arteconi, N. J. Hewitt, and F. Polonara. State of the art of thermal storage for demand-side management. *Applied Energy*, 93:371–389, 2012. doi: 10.1016/j.apenergy.2011.12.045.

Bundesnetzagentur. EEG-Förderung und -Fördersätze: anzulegende Werte für Solaranlagen. https://www.bundesnetzagentur.de/DE/Fachthemen/ElektrizitaetundGas/ErneuerbareEnergien/EEG_Foerderung/start.html, 2026a. Accessed 17 August 2026.

Bundesnetzagentur. Individuelle Netzentgelte Strom gemäß § 19 StromNEV. https://www.bundesnetzagentur.de/DE/Beschlusskammern/BK04/BK4_71_NetzE/BK4_71_Ind_NetzE_Strom/BK4_Ind_NetzEntg_Strom.html, 2026b. Accessed 17 August 2026.

Bundesrepublik Deutschland. Gesetz zur Änderung des EnWG zur Änderung der Vorschriften zur Stromerzeugung aus erneuerbaren Energien ("Solarspitzengesetz"). https://www.gesetze-im-internet.de/eeg_2014/__51.html, 2025. Accessed 17 August 2026.

Bundesrepublik Deutschland. Gebäudeenergiegesetz (GEG), Anlage 9 — Umrechnung in Treibhausgasemissionen. https://www.gesetze-im-internet.de/geg/anlage_9.html, 2026a. Accessed 17 August 2026.

Bundesrepublik Deutschland. Stromnetzentgeltverordnung (StromNEV), § 19 Abs. 2 Satz 1. https://www.gesetze-im-internet.de/stromnev/__19.html, 2026b. Accessed 17 August 2026.

Bundesrepublik Deutschland. Stromsteuergesetz (StromStG), § 9b. https://www.gesetze-im-internet.de/stromstg/__9b.html, 2026c. Accessed 17 August 2026.

Aron P. Dobos. PVWatts version 5 manual. Technical Report NREL/TP-6A20-62641, National Renewable Energy Laboratory, 2014. https://docs.nrel.gov/docs/fy14osti/62641.pdf, accessed 25 August 2026.

Thibaut Esence, Arnaud Bruch, Jean-François Fourmigué, and Benoit Stutz. A versatile one-dimensional numerical model for packed-bed heat storage systems. *Renewable Energy*, 133:190–204, 2019. doi: 10.1016/j.renene.2018.10.012.

Fraunhofer ISE. Energy-Charts — API für Day-Ahead-Preise und öffentliche Nettostromerzeugung. https://api.energy-charts.info, 2026. Accessed 17 August 2026.

Alan C. Hindmarsh, Peter N. Brown, Keith E. Grant, Steven L. Lee, Radu Serban, Dan E. Shumaker, and Carol S. Woodward. SUNDIALS: Suite of nonlinear and differential/algebraic equation solvers. *ACM Transactions on Mathematical Software*, 31(3):363–396, 2005. doi: 10.1145/1089014.1089020.

William F. Holmgren, Clifford W. Hansen, and Mark A. Mikofski. pvlib python: a python package for modeling solar energy systems. *Journal of Open Source Software*, 3(29):884, 2018. doi: 10.21105/joss.00884.

Evangelos Kyritsis, Jonas Andersson, and Apostolos Serletis. Electricity prices, large-scale renewable integration, and policy implications. *Energy Policy*, 101:550–560, 2017. doi: 10.1016/j.enpol.2016.11.014.

Matthias Rehfeldt, Tobias Fleiter, and Felipe Toro. A bottom-up estimation of the heating and cooling demand in European industry. *Energy Efficiency*, 11:1057–1082, 2018. doi: 10.1007/s12053-017-9571-y.

Steffen Schlömer, Thomas Bruckner, Lew Fulton, Edgar Hertwich, Alan McKinnon, Daniel Perczyk, Joyashree Roy, Roberto Schaeffer, Ralph Sims, Pete Smith, and Ryan Wiser. Annex III: Technology-specific cost and performance parameters. In O. Edenhofer et al., editors, *Climate Change 2014: Mitigation of Climate Change. Contribution of Working Group III to the Fifth Assessment Report of the Intergovernmental Panel on Climate Change*, pages 1329–1356. Cambridge University Press, Cambridge, United Kingdom and New York, NY, USA, 2014.

Stadtwerke Jülich. Netznutzungsentgelte nach StromNEV, gültig ab 1.1.2025. Preisblatt, https://netz.stadtwerke-juelich.de/fileadmin/SW-Juelich/user_upload/Netze/NNE_S_2025.pdf, 2025a. Accessed 25 August 2026.

Stadtwerke Jülich. Hochlastzeitfenster für das Jahr 2025 im Elektrizitätsverteilnetz der Stadtwerke Jülich GmbH. Veröffentlichung nach § 19 Abs. 2 StromNEV, https://netz.stadtwerke-juelich.de/fileadmin/SW-Juelich/user_upload/Netze/HLZF_2025.pdf, 2025b. Accessed 25 August 2026.

Statistisches Bundesamt (Destatis). Erdgaspreise für Nicht-Haushaltskunden, 1. Halbjahr 2025. GENESIS-Online, Tabelle 61243-0014, https://genesis.destatis.de/datenbank/online/statistic/61243/table/61243-0014, 2025. Accessed 17 August 2026.

Patrick Zippenfenig. Open-Meteo.com weather API. Zenodo, https://doi.org/10.5281/zenodo.7970649, 2023. Accessed 17 August 2026.

Stefan Zunft, Matthias Hänel, Michael Krüger, Volker Dreißigacker, Felix Göhring, and Eberhard Wahl. Jülich Solar Power Tower—experimental evaluation of the storage subsystem and performance calculation. *Journal of Solar Energy Engineering*, 133(3):031019, 2011. doi: 10.1115/1.4004358.